

High-Fidelity Multiphysics FCEV bus study with detailed HVAC, cabin, and Hydrogen Fuel Cell models

Theodor Ensburly¹ Alessandro Picarelli² Mike Dempsey²

¹Claytex USA, Inc., United States, theodor.ensburly@claytex.com

²Claytex Services Ltd. Edmund House, Rugby Road, Leamington Spa, CV32 6EL, UK,
{alessandro.picarelli,mike.dempsey}@claytex.com

Abstract

Hydrogen Fuel Cells are potentially a viable zero emission propulsion technology for heavy commercial vehicles, like buses. This paper presents a detailed proof of concept Dymola model of an FCEV bus, built using the VeSyMA suite of libraries. Particular attention is paid to the use of the high-fidelity Hydrogen Library from Dassault Systèmes for the fuel cell. Representative physical ancillary systems, coupled with detailed thermochemical modelling, enables detailed transient effects on fuel cell performance to be captured. A multizonal cabin model with independent zonal thermal properties, combined with a multi-physics HVAC model provide a realistic current drain on the drive battery. Such detail is important in understanding accurately the conditions the Fuel Cell will experience during operation. A model such as this has many real-world applications, such as component design and selection; concept evaluation; Fuel Cell degradation, maintenance, and durability analysis; accurate range estimation and controller development.

Keywords: Hydrogen, Fuel Cell, HVAC, heating, cooling, bus, coach, EV, FCEV

1 Introduction

Due to the impact of global warming and air quality standards, internal combustion engine (ICE) driven vehicles are being phased out of usage. Passenger Electric Vehicles (EVs) are becoming the norm. Many markets have established sunset dates for the sale of ICE vehicles, triggering the development of electrified vehicles en masse, as intended.

The energy source for this electricity is still a cause for debate. Battery Electric Vehicles (BEVs) have emerged as the dominant technology for passenger vehicles. Such vehicles feature a solid-state electrochemical battery, usually of lithium-ion technology. As commercial vehicles are often in constant use during operational hours, the range limitations of BEVs and time it takes to recharge them, compromise their suitability for commercial applications (Andaloro et al, 2016). A comparatively low energy density of modern EV battery technology versus Hydrogen plays a role in this, with Fuel Cell

Electric Vehicles (FCEVs) more suitable, capable of driving ranges greater than 300 miles (Gröger et al, 2015). Procurement of the rare earth minerals needed for BEV batteries also presents its own set of ethical and environmental supply chain concerns (United Nations, 2020).

Transit and coach buses present an interesting use case. In continuous operation during the day, transit buses stop frequently, albeit for very short periods to allow passengers to embark and disembark. In contrast, coach buses stop infrequently, but often travel long distances in a single journey. Neither present a natural use case for the pure BEV concept.

Hydrogen fuel cells (FCs), when powered with green hydrogen, present a potential solution to this predicament. FCEV buses offer a comparable range and can be considered a “one for one” replacement for existing diesel buses (Vock, 2019). Refueling times are and equivalent fuel efficiency are comparable with current diesel-powered vehicles (Eudy and Post, 2021); some manufacturers already claim comparable range and performance to conventional ICE buses (Luxfer, 2022).

1.1 Motivations for study

Beyond reducing the carbon footprint of development by eliminating almost all prototypes, simulation tools feature heavily in vehicle electrification. The multi-physics capability of modern simulation tools and languages such as Dymola and Modelica, are ideally suited to simulating the EV, an inherently complex multi-physics system. Motivations for this study can be broadly broken down into two concepts: theoretical and practical.

Initially undertaken as a technical exercise, from a theoretical perspective this work follows common themes. Primarily, it serves as a proof of concept with regards to integrating the Vehicle Systems Modelling and Analysis (VeSyMA) suite of vehicle simulation libraries from Claytex and the Hydrogen library from Dassault Systèmes (DS). Work stemming from the development of this model was directly responsible for the adaptation of the VeSyMA library to interface with the Hydrogen library.

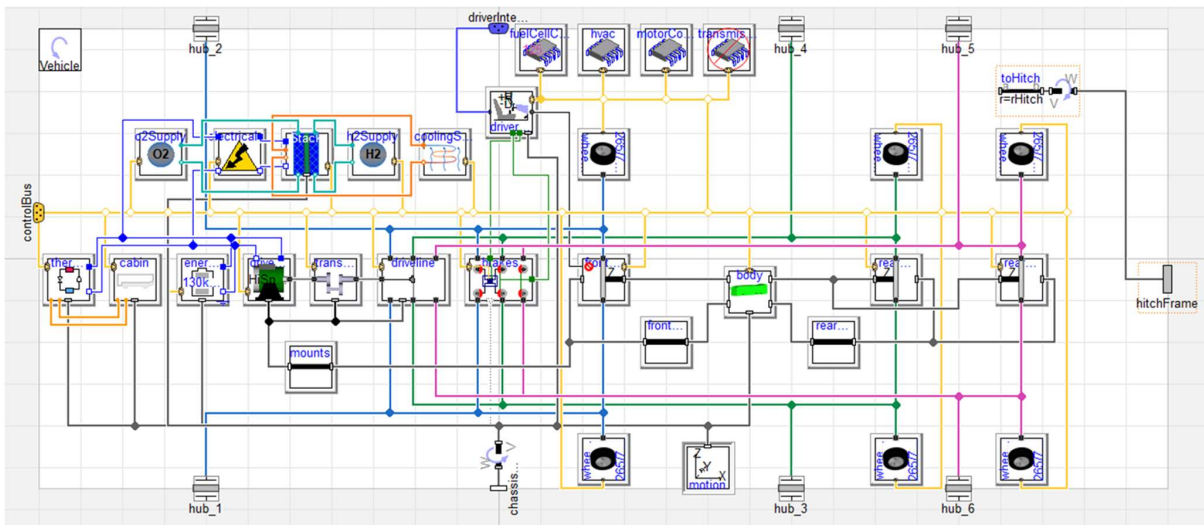


Figure 1 - FCEV Bus model by Claytex. Following the VeSyMA principles, a template system to promote model reuse and replaceability is used, allowing for scalable detail. Note the Fuel Cell components in the top left-hand corner, and the Cabin and HVAC models on the far left-hand side.

On a practical level, there are several real-world benefits. Featuring high fidelity HVAC and FC models, it can be used to accurately size, design and select components for usage and evaluate their suitability in the digital twin. Cooling needs of the FC can be evaluated with regards to the loading cycles it undergoes; needs and benefits of preconditioning can also be determined with a model such as this. With a detailed HVAC and cabin model, the FC in the model operates in realistic, and sometimes compromised, loading conditions. As FCs are very sensitive to operating conditions, the bus model presented can be used as a plant model for controller development. Beyond this, the lifecycle and potential degradation and durability of the FC can be understood; important when optimizing control systems and strategies. Finally, such a model also gives an accurate picture of the potential range and performance of the vehicle, useful in validating a design's effectiveness prior to prototyping.

2 Modelling

The bus model described in this paper was created as an example model for the Vehicle Demos library from Claytex. This library is a showcase, demonstrating how the VeSyMA suite can be interfaced with external third-party libraries (Hammond-Scott and Dempsey, 2018).

In this case, the bus model was created from components and templates in the VeSyMA library, whilst integrating a cabin and HVAC model from the Thermal Systems library from TLK, along with fuel cell components and stack model from the Hydrogen library by Dassault Systèmes. Kormann and Krüger (2019) have elaborated on some of the principles underpinning the Hydrogen library.

2.1 Bus Model

In FCEV applications, the fuel cell itself is mounted in a series configuration; primarily used to replenish a drive battery, which ultimately delivers electricity to the drive motors. Applications of FC technology to buses seem to follow the same logic, with both Tata Motors (Yogesha et al, 2019) and Toyota (Ogawa et al, 2019) producing buses of this type for use in transit scenarios.

Ogawa (2019) describes how originally in 2002, Toyota produced a FCEV bus using a single fuel cell coupled to a single battery, to drive a single motor unit. Sugiura (2016), describes a dual fuel cell bus, where a single battery per fuel cell was used. Later in 2019, a second-generation FCEV bus was presented by Toyota, this time featuring twin fuel cells allied to a pair of batteries in this case. Yogesha (2019) indicates that Tata Motors have taken another approach, coupling a single fuel cell to dual drive batteries and motors units.

Deciding on the optimal layout requires balancing, component mass, size, packaging ability, thermal management, and performance. Twin stacks and batteries would be easier to package, although potentially less efficient. Dual batteries could be a solution to the packaging problem. Simulation is the perfect tool to evaluate this before committing resources and effort to prototyping. As ultimate performance was not the goal, a simple layout of a single fuel cell coupled to a single drive battery was chosen.

Whilst the bus model chassis itself has full multibody capabilities; the purpose of this exercise was to investigate the longitudinal performance of the vehicle power train. Therefore, the principles established in the VeSyMA library simplifying the vehicle dynamic degrees of freedom (DOF) were followed. This means the suspension utilized was rigid as the bus traversed a

perfectly flat road model, with the total motion of the model constrained to 3DOF (translational x, rotational y and translational z) to improve simulation performance. Similarly, tyre modelling was limited to linear longitudinal slip, of a 26570/R19.5 size.

Of note, the bus model featured 3 axles, as is commonly encountered with bus type vehicles, one at the front and two at the rear. Drive was supplied directly to the middle (first rear) axle through an ideal open differential model. A 550Nm mapped motor model was used which included the mass and inertia of the stator and core. Finally, a 130kWh idealized battery model was deployed, with varying output voltage and a fixed internal resistance. It is important to note that review of literature suggests that this battery size is too large for a FCEV bus; it is equipped with this battery to enable comparison with the existing pure EV bus model found in the Vehicle Demos library, as presented in section 3 of this paper.

2.2 Fuel Cell Model

The Fuel Cell model is broken down into 6 subcomponents, mimicking the described layouts found in the aforementioned literature. They are:

- Stack
- Anode hydrogen supply system
- Cathode air supply system
- Cooling system
- Boost Converter Circuit
- Control system

Each subsystem occupies a single model slot at the top level of the bus vehicle model. This continues the principle of component “plug and play” replaceability established in the VeSyMA library. All fluid modelling components used in these models are taken from the Hydrogen library; valve and pipe models are included, featuring representative pressure losses across them. Note, thermal rejection to surrounding components from transport elements are neglected in this study, but the model is equipped to include those effects if desired by the user. These effects were neglected in this study owing to the lack of a representative system to base the model upon.

At the heart of the Fuel Cell model (Figure 2) is the stack model. Taken from the Hydrogen library, the stack used is a Proton-Electron Membrane (PEM) parameterised with a polarization curve from 125KW PowerCell S3 Fuel Cell stack. Defined in the Hydrogen Library as a *stackWithCooling_DetailedMembrane*, this stack model simulates the current generation of the stack, fully dependent upon the temperature and pressure of the reactants in the Anode and the Cathode. The effect of humidity on the stack performance is omitted in this model. A thermal model built into the stack enables the effect of fluid cooling to be incorporated into the performance of the stack. Moving

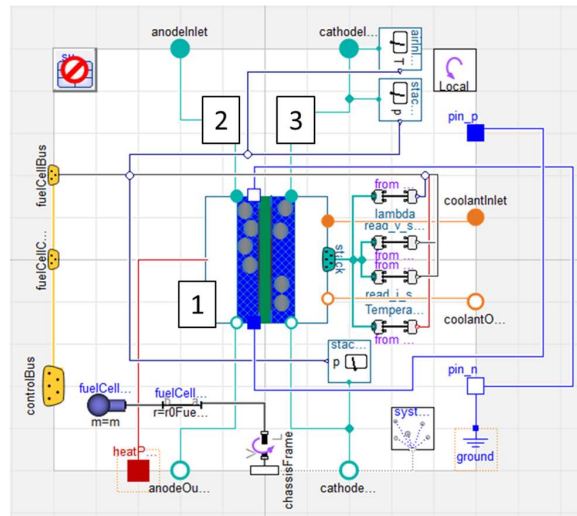


Figure 2 - Fuel Cell stack model. The Electrochemical stack model is deployed with signal routing, connector interface and mass properties, enabling it to feature in the multibody bus model. Note: stack (1), anode (2) and cathode (3).

onto the hydrogen supply system for the stack anode (Figure 3), hydrogen flow is modelled from a fuel tank through a recirculation loop with the anode. Supply pressure is maintained via a valve dependent upon a control signal from the controller model. Hydrogen passes through a humidifier before entering the recirculation loop. To recirculate the hydrogen, a ThomasGardner 907ZC18 pump performance map is used, upscaled 20x to meet the demand of a more powerful stack. Finally, a purge valve on the exit of the loop is controlled to maintain the mass fraction of oxygen in the anode fluid to be less than 0.1.

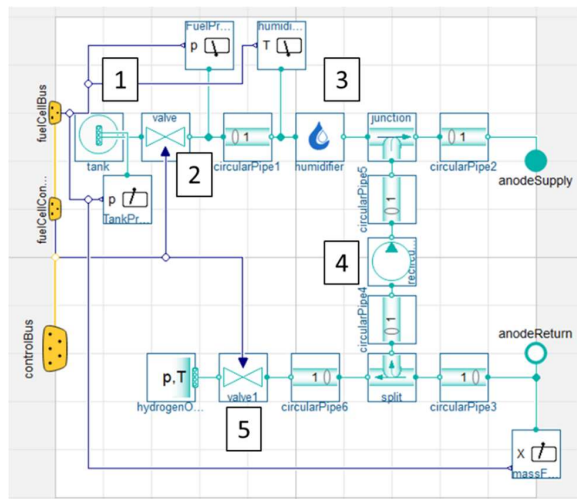


Figure 3 - Hydrogen supply model with recirculation system. Note: hydrogen tank (1), fuel pressure valve (2), humidifier (3), recirculation pump (4) and purge valve (5).

For the air supply system to the stack cathode (Figure 4), a similar modelling philosophy is employed. Here, a model of a Celeroton CT17 700 compressor with efficiency and pressure ratio map is used to compress ambient air; compressor speed is driven via a control signal from the controller. Upon exiting the compressor, the air moves through a heat-exchanger (effectiveness-NTU method) intercooler, to reject heat generated from compression to a 1,2 Propylene Glycol 47% water mix coolant flow, controlled via a command signal. Compressed, cooled air passes through a humidifier before entering the cathode. After passing through the stack, the exhaust flows through a water extractor. This has been included to account for the pressure drop across it due to this commonly used component. Finally, the pressure across the stack is governed by an exhaust valve, once again driven via command signal from the controller.

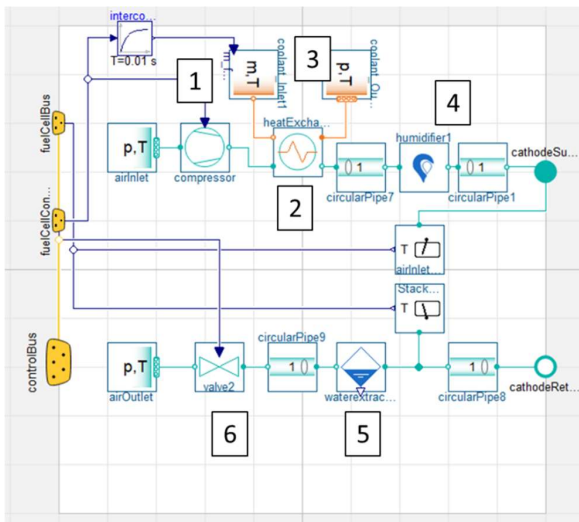


Figure 4 - Air supply system. Note the heat exchanger used to cool the oxidant feed post compression. As the stack model incorporates thermal effects regarding reaction suitability, then a temperature correct oxidant feed is required. Note: air compressor (1), heat exchanger (2), coolant supply (3), humidifier (4), water extractor (5), exhaust valve (6)

In comparison to other elements of the Fuel Cell model, the cooling and electrical components are simplified. A 1,2 Propylene Glycol 47% water mix coolant flow is specified by the controller model. Flow is regulated to maintain the stack at a specific temperature level. No pumping dynamics or losses are included at this time. Voltage generated by the stack is scaled via a constant efficiency DC/DC boost converter to step up the voltage delivered to the drive battery. A demanded current is used to control the stack output using this component.

The last element of the fuel cell model is the controller responsible for governing the system. This has been broken down into 5 subsystems; one each for

the cooling, electrical, air and fuel subsystem models described above, and a state controller. A set of logic gates based on the stack temperature, fuel tank pressure, stack current, stack voltage and battery state of charge determine the stack’s state within a rudimentary state machine with 3 modes; “startup”, “normal running” and “shut down”. This has been designed to enable the stack to enter a “shut down” mode if it exceeds safe operating conditions, fuel supply is diminished, or the battery exceeds a maximum charge threshold to preserve fuel supply. At the time of writing the controller has only been tested in the normal running state.

In terms of actual control signals, a PID approach is used. Cooling demand for intercooler is driven by PID with a target of 50°C, with the stack system having a target of 45°C. A 2D lookup table, dependent on driver torque demand and battery state of charge defines the stack current demand. Intake air compressor is driven by a scalable lambda value of the stack; lambda being the ratio of provided to used oxygen in the stack. Cathode exhaust valve opening is controlled relative to the pressure differential across the inlet/outlet from the stack, with a target difference of 0.5bar. Fuel supply pressure from the tank is maintained at 3.2bar during normal running conditions. The hydrogen purge valve is modulated to keep the mass fraction of oxygen in the anode side of the stack below 0.1.

2.3 Cabin and HVAC Model

The cabin model (Figure 5) is a multi-zone cabin model with partitions including glazing, solid partitions, and internal furniture. The cabin/compartment model is split into front, middle and rear zones and can have a variable number of passengers within it. The orientation or bearing of the compartment influences the angle at which the solar radiation hits the external partitions which affects the thermal loading on the partitions and interior of the compartment.

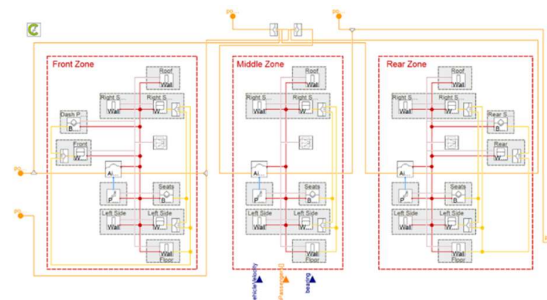


Figure 5 - Multi-zone cabin model with unique elements, such as furniture and glazing properties. The front has a large frontal windshield and dashboard thermal mass, the middle zone has opening doors.

The HVAC model (Figure 6) uses an electrically driven compressor to pump the R134a refrigerant around the two-evaporator, one-condenser system. The electric

motor for the compressor uses electrical power from the traction battery via a voltage regulator. Each evaporator branch has its own thermal expansion valve which is independently controlled to achieve a desired superheat value of the refrigerant flowing out of each evaporator.

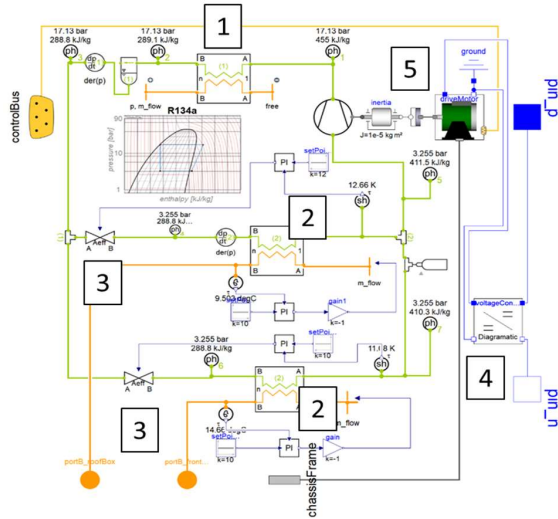


Figure 6 - HVAC model. Note the individual condenser models. Note: condenser (1), evaporators (2), expansion valves (3), voltage regulator (4) and motor (5).

3 Testing & Evaluation

As this paper is concerned with the demonstration of the functioning of the Hydrogen library, Thermal Systems library and VeSyMA, control parameterisation has been geared towards exercising the model rather than replicating a realistic usage. The FCEV bus results are also compared to the EV only version of this bus model found in the Vehicle Demos library, identical as figure 1 minus the FC; to make the comparison valid, the EV bus was also equipped with the same 130KW battery model as the FCEV.

3.1 Drive Cycle Scenario

The Standardized On Road Test (SORT) suburban drive cycle for bus applications is used, as per Figure 7.

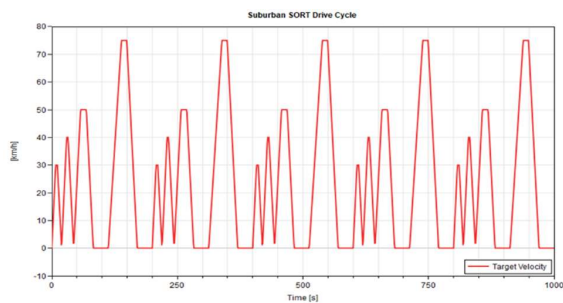


Figure 7 - SORT Suburban drive cycle used to test the bus model.

3.2 Results

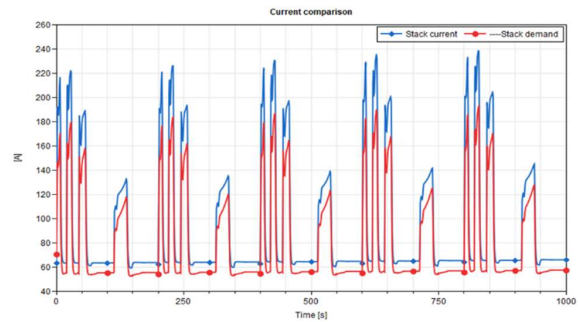


Figure 8 - Current comparison between demand and result. The modulus of the demand current was used for comparisons sake. Blue is stack current, red stack demand.

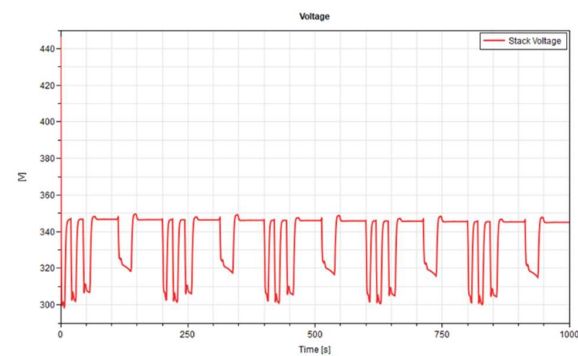


Figure 9 - Voltage produced by the stack.

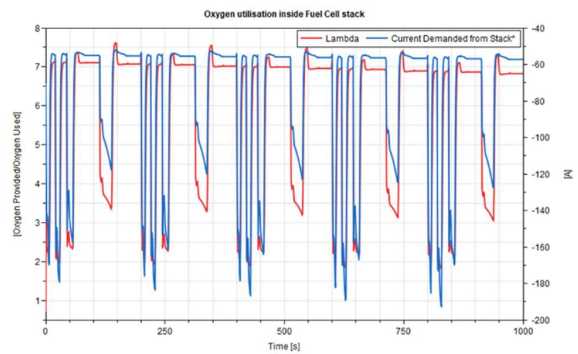


Figure 10 - Oxidant usage in the stack cathode. Red is Lambda, blue the current demand from the stack.

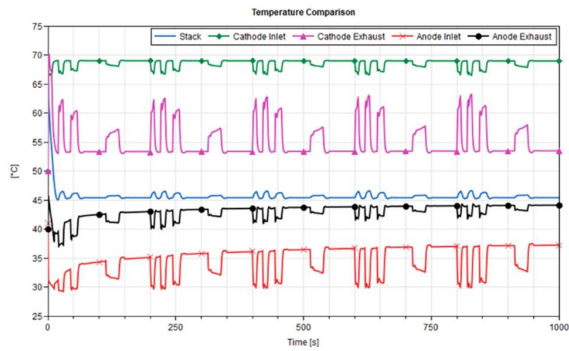


Figure 11 - Temperature comparison across the stack. General stack temperature is blue, the cathode inlet green, cathode exhaust magenta, anode inlet orange and the exhaust black.

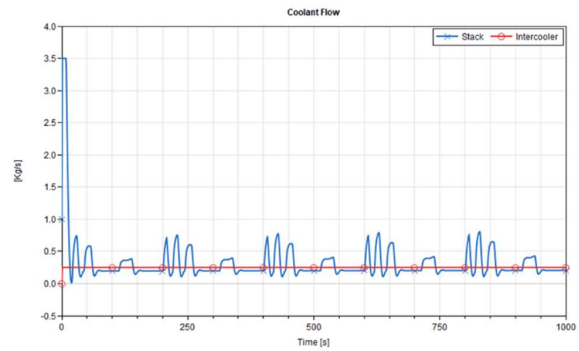


Figure 14 - Coolant flow into the stack (blue) and the intercooler (red).

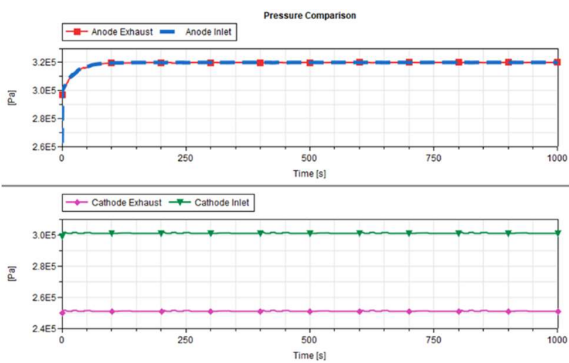


Figure 12 - Pressure comparison across the stack. Anode exhaust is red and the inlet blue; cathode exhaust is magenta and the inlet green.

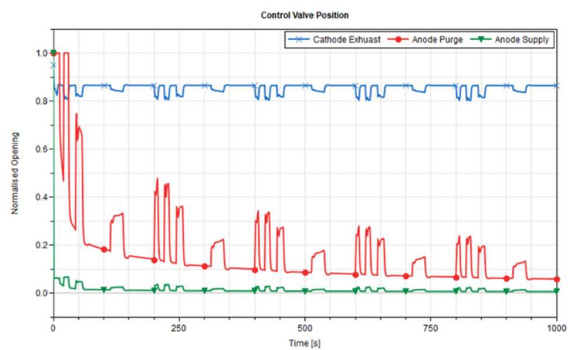


Figure 13 - Control valve position. Large initial transients to steady state can be corrected with improvements to the stack initial conditions. Blue is the cathode exhaust valve, red the anode exhaust valve and green the anode supply valve.

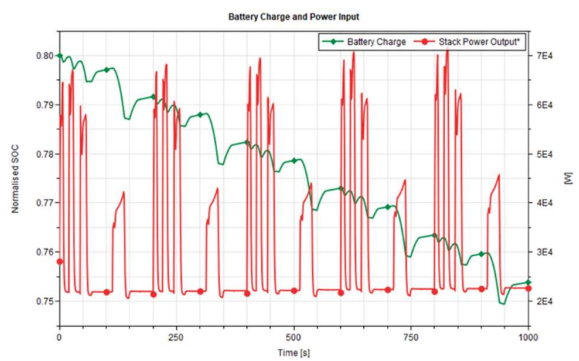


Figure 15 - Battery power input (red) and effect on state of charge (green).

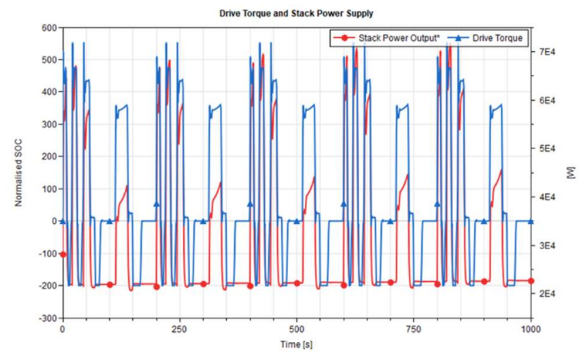


Figure 16 - Stack power output (red) relationship to drive torque (blue).

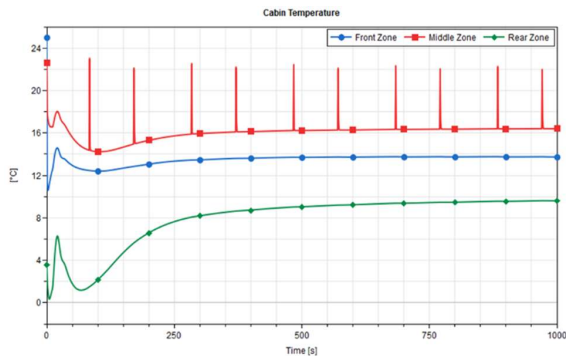


Figure 17 - Cabin temperature in each of the 3 zones; front (blue), middle (red) and rear (green).

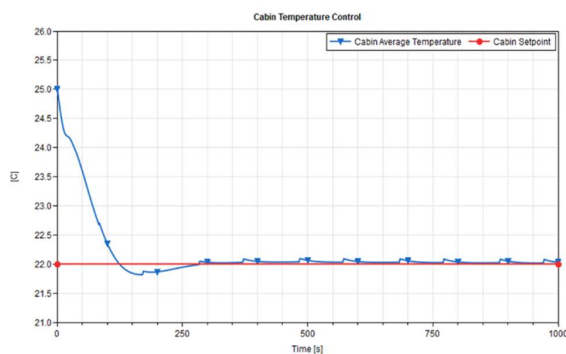


Figure 18 - Temperature control of the cabin. Cabin temperature is blue, the setpoint in red.

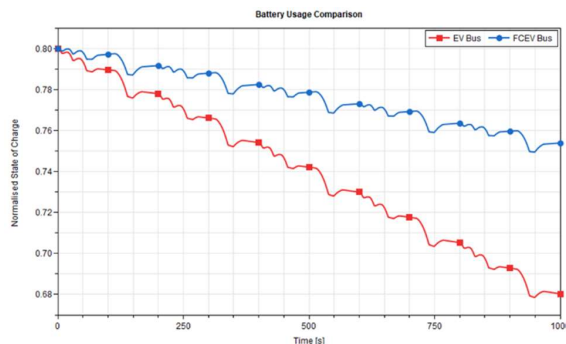


Figure 19 - Comparison between the SOC of the battery in comparable FCEV (blue) and BEV (red) bus models.

3.3 Discussion of results

As the SORT drive cycle was specifically designed for evaluating bus driveline performance, it gives some interesting insights into the FCEV Bus model. Immediately from Figure 8, the fuel cell is responding well to the current demanded from it. There is little response lag, suggesting the ancillary and control systems are working well and keeping the fuel cell in a desired operational window. Fast response to current reduction indicates that the choice to control the fuel cell via current demand was valid, as there is no delay in current reduction from the fuel cell. Detail around the peaks of the current response mirroring the demand indicates the fidelity of the model being used, able to react swiftly. Such detail would be important when trying to evaluate the total range/fuel consumption of the cell. It must be noted however, that the fuel cell is exceeding the current demand; this can likely be remedied with improved controller parameterisation. Voltage time history in Figure 9 supports the conclusions drawn from Figure 8, also indicating there is a slight overshoot in fuel cell voltage as the current demand is removed. Fidelity is further demonstrated by Figure 10, with fluctuations in current demand evident in the oxygen concentration in the cathode. Lambda spikes to a higher value than the steady state after current demand is reduced suggesting a degree of actuator hysteresis, likely in the compressor control.

Comparing the temperature of the stack itself and the gaseous mixtures in the inlet/exhaust of the stack anode and cathode in Figure 11 indicates a global level of settling of temperatures to a steady state, most likely because of unoptimized simulation start values. Once again, they fluctuate with demand.

Generally, we see heat flows from the cathode to the anode side, with the cathode exhaust losing temperature and the anode exhaust gaining it relative to their respective intakes.

Interestingly, the instantaneous temperature fluctuations found in the cathode exhaust relative to the inlet are lessened in the anode. One could deduce that this could be a result of the differing thermal inertias of the gaseous mixtures themselves, although a more likely explanation is that the cathode side features an exhaust valve to atmosphere; the anode system features a hydrogen recirculation system and a purge valve. As the cathode system is more sensitive to the volumetric change, comparatively the cathode side gas will be subject to a larger temperature increase due to compression as the valve closes.

Cross referencing with Figure 13 supports this hypothesis, as both the anode purge and the cathode exhaust valves are overshooting the target somewhat, but it is only the cathode gases experiencing a momentary temperature spike. Essentially, the cathode

exhaust valve closes too much and then opens a little as the system dynamics settle. Tuning of the controllers will remedy this.

Owing to a greater thermal inertia of the stack itself, overall stack temperature fluctuations are more muted than the anode and cathode gases. This is entirely expected.

Figure 12 indicates that the 3 control valves, cathode exhaust, anode purge and hydrogen supply, are behaving broadly as they should to manage the pressure within the stack. Pressure fluctuations are minimal, but a cursory glance at Figure 13 does reveal some overshoot and further investigations reveals some interesting insights about the system dynamics. Hydrogen supply is increased due to demand; the purge valve also opens more during demand events, indicative of a greater oxygen concentration in the anode as more reaction takes place. The action of the cathode exhaust valve corroborates this, as it is closing slightly during demand events; this will be to maintain pressure across the cathode, indicating a pressure drop of some kind. Therefore, it appears that there is gaseous loss towards the anode. The temperature gradient identified previously from the cathode inlet to the anode exhaust supports a theory of gaseous loss towards the anode in this manner.

Figure 14 indicates an opportunity to improve the air compressor control. The constant flow of coolant into the intercooler and the stability of the cathode inlet temperature (during steady state low current demand) belies a compressor which is running at a constant speed. This explains why the Lambda value spikes when there is little current demand; instead of reducing speed when there is little load, it continues at a constant speed. Stack coolant flow positively correlates with greater heat generation due to demand.

Reviewing Figure 15 and 16, we can make some conclusions as to how the overall logic of the electrical controller, responsible for the current demand from the stack, is functioning. Current demand is rising and falling rapidly; this is due to the controller being parameterised to only demand current continuously when the battery SOC drops below a certain threshold. Therefore, as Figure 16 proves, the fuel cell is only engaging fully in heavy tractive events. This is an expected outcome, as the deployment strategy was inspired by Ogawa (2019), who proposed the use of a Fuel Cell demand override during strenuous tractive events, to reduce battery size. It should be noted that the maximum power produced by the stack does not reach the stated maximum rating. Improvements to the controller logic given the battery SOC are likely to remedy this, by improving the running conditions of the stack.

Figures 17 and 18 indicate that the cabin thermal and HVAC models are performing as intended. The air inlet compromising the cabin doors is connected to the

middle zone of the cabin, as described in Figure 5. With an outside air temperature of 30°C, this means a volume of warm air is admitted to the cabin; the HVAC system, has a setpoint of 22°C. We see that the middle zone temperature spikes when the cabin doors are opened, letting warmer air into the volume. Whilst this causes the middle section to increase in temperature alone versus the front and rear, Figure 18 demonstrates how it increases the average temperature. Action of the HVAC system then returns the temperature to the setpoint.

Finally, Figure 19 demonstrates the positive effect of the fuel cell on the battery charge, versus a comparable EV bus with no fuel cell. Whilst it is true that the battery deployed in the FCEV is much larger in capacity relative to numbers disclosed in published literature by Toyota and Tata, it nevertheless serves as a reminder of the advantages of a FCEV versus a pure EV in such situations.

4 Conclusions

Overall, it can be concluded that the FCEV bus model presented in this paper is functioning in a valid way as a proof of concept. Useful observations regarding the interplay of the control system, which has 3 elements (hydrogen supply to the anode, air supply to the cathode and current demand) to manage can be made. We can see the model is sensitive to small control changes, in a logical way. Such sensitivity is important, as it encompasses all the systemic nonlinearities that a controller or physical system must manage. This gives confidence to using such a model in place of a real-life prototype. As discussed, there is scope to further improve the simulation with optimization of the control parameters. Nevertheless, it has been useful to exercise the system and observe the trends and dynamics.

4.1 Further Work

The most immediate improvement that could be made to the model would be to deploy the *stack_MembraneDetailedHumidity* stack model, to include the effect of humidity directly on the current produced by the fuel cell. One advantage of a detailed model such as the one presented in the paper is the ability to study the coupled thermodynamic effects; all the transport components such as pipes in this model have the capability to include thermal heat transfer to the boundary. Coupled phenomena regarding the design of the bus could be studied. Such a case would be the effect of the HVAC system running during hot weather, with the addendum potential for a greater current demand from fuel cell. Preconditioning studies could also be conducted, a feature which literature shows potential for improving the range of conditions a fuel cell can operate. Cold conditions specifically are of interest, as they traditionally impact BEV performance greatly. Further studies into fuel cell management and lifecycle

could be conducted, especially the case of dosing water management, if physical water capture, use and recycling is added to the model. Further insight into the specific infrastructural requirements needed to support Hydrogen buses could be understood by doing this.

Acknowledgements

The authors would like to thank Imke Lisa Krüger and Markus Andres of Dassault Systèmes for their assistance in using the Hydrogen library components in this model.

References

- L. Andalaro, S. Micari, G. Napoli, A. Polimeni and V. Antonucci (2016). A hybrid electric fuel cell minibus: drive test. *EVS29 International Battery, Hybrid and Fuel Cell Electric Vehicle Symposium*. World Electric Vehicle Journal. 2016, 8(1), 131-138; <https://doi.org/10.3390/wevj8010131>
- L. Eudy and M. Post. 2021. Fuel Cell Buses in U.S. Transit Fleets: Current Status 2020. Golden, CO: National Renewable Energy Laboratory. NREL/TP-5400- 75583. <https://www.nrel.gov/docs/fy21osti/75583.pdf>.
- O. Gröger, H. A. Gasteiger, and JP. Suchsland. Review – Electromobility: Batteries or Fuel Cells? *Journal of the Electrochemical Society*. 162 (14) A2605-A2622 2015. DOI: 10.1149/2.0211514jes
- H. Hammond-Scott and M. Dempsey (2018). Vehicle Systems Modelling and Analysis (VeSyMA) Platform. *Proceedings of the 2nd Japanese Modelica Conference, 2018*. DOI: 10.3384/ecp18148
- M. Kormann and I. L. Krüger (2019). Application of a Real Gas Model by van der Waals for a Hydrogen Tank Filling Process. *Proceedings of the 13th International Modelica Conference, 2019*. DOI: 10.3384/ecp19157665
- Luxfer Gas Cylinders. 2022. *Hydrogen Buses*. Online. Accessed 1st August 2022. Available at: <https://www.luxfercylinders.com/news/hydrogen-buses#:~:text=On%20average%2C%20a%20hydrogen%20bus,ride%20is%20smoother%20and%20quieter.>
- T. Ogawa, K. Umayahara and Y. Ikogi (2019). Development of Fuel Cell (FC) System for New Generation FC Bus. *SAE International Journal Advances & Current Practice in Mobility* 1(2):782-786, 2019, doi:10.4271/2019-01-0372.
- T. Sugiura, A. Tanida, and K. Tamura (2016). *Efficiency Improvement of Boost Converter for Fuel Cell Bus by Silicon Carbide Diodes*. *SAE International Journal Alternative Powertrains*. 5(2):2016, doi:10.4271/2016-01-1234.
- United Nations. 2022. *UN Highlights urgent need to tackle impact of likely electric car battery production boom*. Accessed 1st August 2022. Available at: <https://news.un.org/en/story/2020/06/1067272>
- D. C. Vock. 2019. *Batteries or Hydrogen? Cities Weigh Making Buses Electric*. Online. Accessed 1st August 2022. Available at: <https://www.govtech.com/products/batteries-or-hydrogen-cities-weigh-the-best-way-for-buses-to-go-electric.html>
- S.A. Yogesha, S. Brahmabhatt, M. Raja, S. Arikapudi, B. Bhut and V. Jalkumar (2019). Development of Hydrogen Fuel Cell Bus Technology for Urban Transport in India. *SAE Technical Paper 2019-26-0092*. 2019, doi:10.4271/2019-26-0092.